BASEMENT GEOMETRY, FROM MAGNETIC AND GRAVITY DATA IN GASTRE TROUGH, CHUBUT, ARGENTINA.

Federico Lince Klinger; M. P. Martinez; M. E. Gimenez; F. Ruiz (IGSV, UNSJ)

Abstract:

A gravimetric and magnetometric study at Gastre Trough, province of Chubut, allowed to reveal its basement geometry. Maps of anomalies show a fractured basement with high and sunk blocks inside the Trough. The minimum anomalous are associated to graben-like depocenters possibly inverted during the Tertiary, while the maximum are linked to basement blocks. Some of these blocks outcropping at the edges of the trough and some others covered by sediments inside. A 3D analytical signal and a gravity horizontal gradient were applied in order to make an appropriate interpretation, associating the maximum magnetic susceptibility changes and density to contacts between different lithologies. Finally, outcropping density values as well as seismic density values allowed to make 2D density models across to the Trough, which showed the presence of a high basement as central Gastre Trough.

Key words: Trough, magnetometric, gravity, geometry, basement.

Introduction

In the extra-andean Patagonia, to the Southwestern North Patagonic Massif, a depression extends northwest - southeast named Gastre Trough (Figure 1). Authors such as Coira et al., (1995) relate the origin of this trough to a transtentional tectonic, product of a course failure reactivation, from Paleozoic to Precambrian ages. This system of fractures along with mylonites strips developed in plutonic rocks from the late Triassic - early Jurassic (Rapela, 1997) in Calcatapul and Lonco Trapial Sierras are the basis of the hypothesis developed by Rapela and Pankhurst (1992). According to Figari (2005) due to the extensive and transtensive efforts the Gastre Trough constitutes a depocenter originated in the middle and upper Jurassic, being later partially inverted by a compressive stage during the Tertiary, constituting along other isolated depocenters the Cañadón Asfalto basin (Figari and Courtade, 1993; Cortiñas, 1996) (Figure 1).

In the mentioned area, the entities from Precambrian to lower Paleozoic stages are known as basement, being this constituted mainly by metamorphic, volcanic and plutonic rocks grouped in the *Formations Cushamen* (Volkheimer, 1964), *Calcatapul* (Proserpio, 1978) y *Mamil Choique* (Ravazzoli y Sesana, 1977) (Figure 1). The *Formation Cushamen´s* shales and the amphibolites, are intruded by the *Formation Mamil Choique´s* mesosilisicas plutonites and by a calc-alkaline granitoids set assigned to *Formation Lipetrén* (Proserpio, 1978), from the late Triassic - early Jurassic (Rapela, 1997). The deposits at Cañadón Asfalto basin, acknowledged in the area of middle Chubut river, represent the different stages of a rift - postrift system. The *Group Lonco Trapial* volcanic-sedimentary sequence (Lesta y Ferello, 1972) and the *Formation Cañadón Asfalto* lower section constituted by levels of limestone, pelites, sands and conglomerates with collations of basaltic lava represent the rift early development stage.

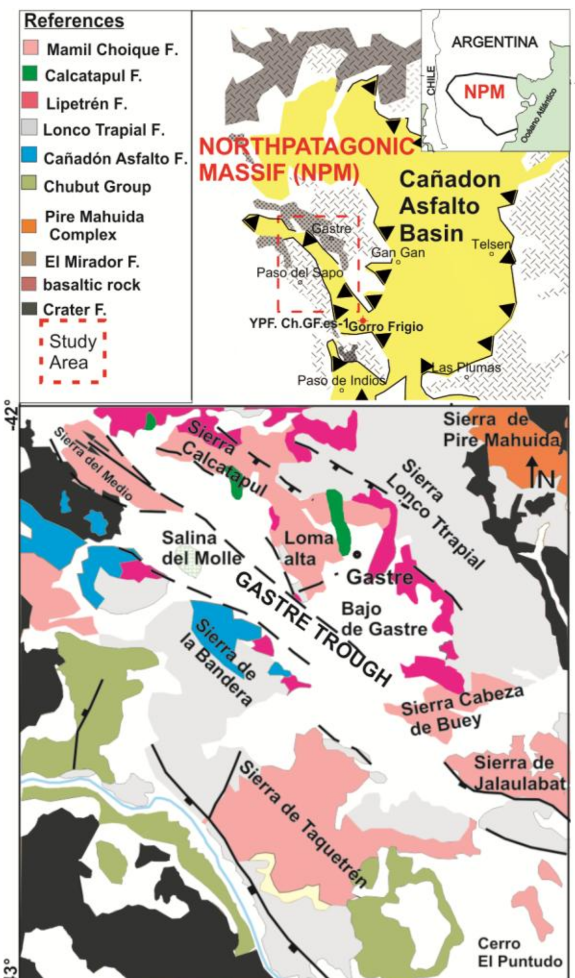

Figure 1: Geological map

The upper section of *Formation Cañadón Asfalto* where sandstone, limonites, pelites and limestone are involved has been assigned by Figari and Courtade (1993) to the final stage of the graben evolution. In the post-rift stage the deposits accumulated during the basin thermal subsidence in the middle reaches of Chubut River have been included in the *Group Chubut* (Lesta, 1968). Group Chubut is divided into two big units, one lower, essentially epiclastic *Formation Los Adobes* (Tasch and Volkheimer, 1970) and an upper one with an important pyroclastic participation *Formation Cerro Barcino* (Nakayama, 1972).

Data acquisition:

Through the use of a Lacoste and Romberg G-981 gravimeter (0.01 mGal precision) and a protonic magnetometer in Gastre, province of Chubut, 572 magnetometric and gravity stations were relieved (Figure 2). In each station the WGS84 (World Geodetic System 84) referred ellipsoidal height, was determined using two geodesic simple frequency and sub-metric precision GPSs. The average error made at the plain-altimeter survey was of 0.32 m, dragging an average error in the calculation of the Bouguer anomaly of 0.1345 mGal.

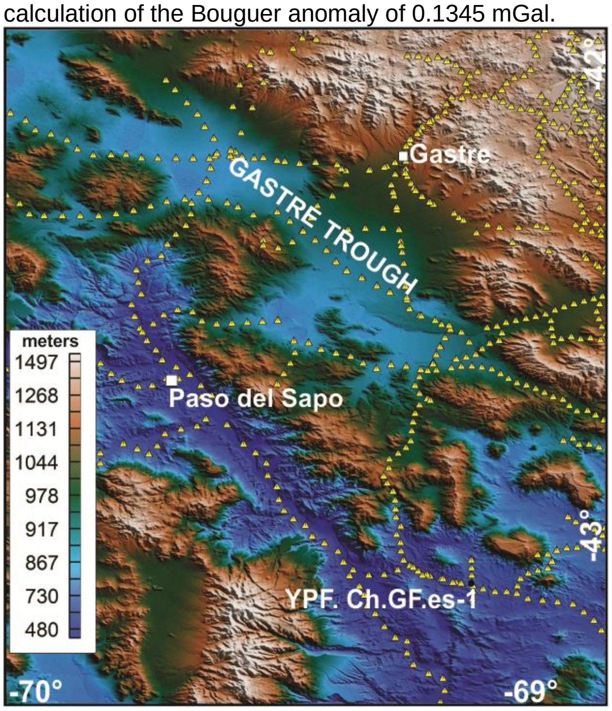

Figure 2: Distribution of gravimetric, magnetometric and topographic stations. Location of YPF Ch GF es -1 well.

Gravity data processing

The gravity readings were corrected via instrumental drift. They were later linked to the Miguelete's fundamental value (Buenos Aires): 979690.03 mGal, first-order station which belongs to the IGN national gravimetric net. Theoretical gravity was calculated according to ellipsoid IGSN71 (International Gravity Standardization Net 1971, Morelli et al., 1974). In the Bouguer's anomaly calculation, the classical gravity formulas were used (Blakely, 1995), considering an average density for 2670 kg m^{-3} rocks (Hinze, 2003). A topographic correction was made with two digital elevation models (DEM): a) Local DEM with a 90 m cell size; b) regional DEM, which expanded 167 km to the outside of the local DEM with a 250 m cell size. Although the models used are ellipsoidal, the error made in the topographic correction is not meaningful due to dimension of the study area (Hinze et al., 2005).

The regional gravimetric effect was obtained using a 3556 gravity data base (Figure 3b) which belong to the Instituto de Física de Rosario (IFIR) and Instituto Geofísico Sismológico Volponi (IGSV) covers a wider area.

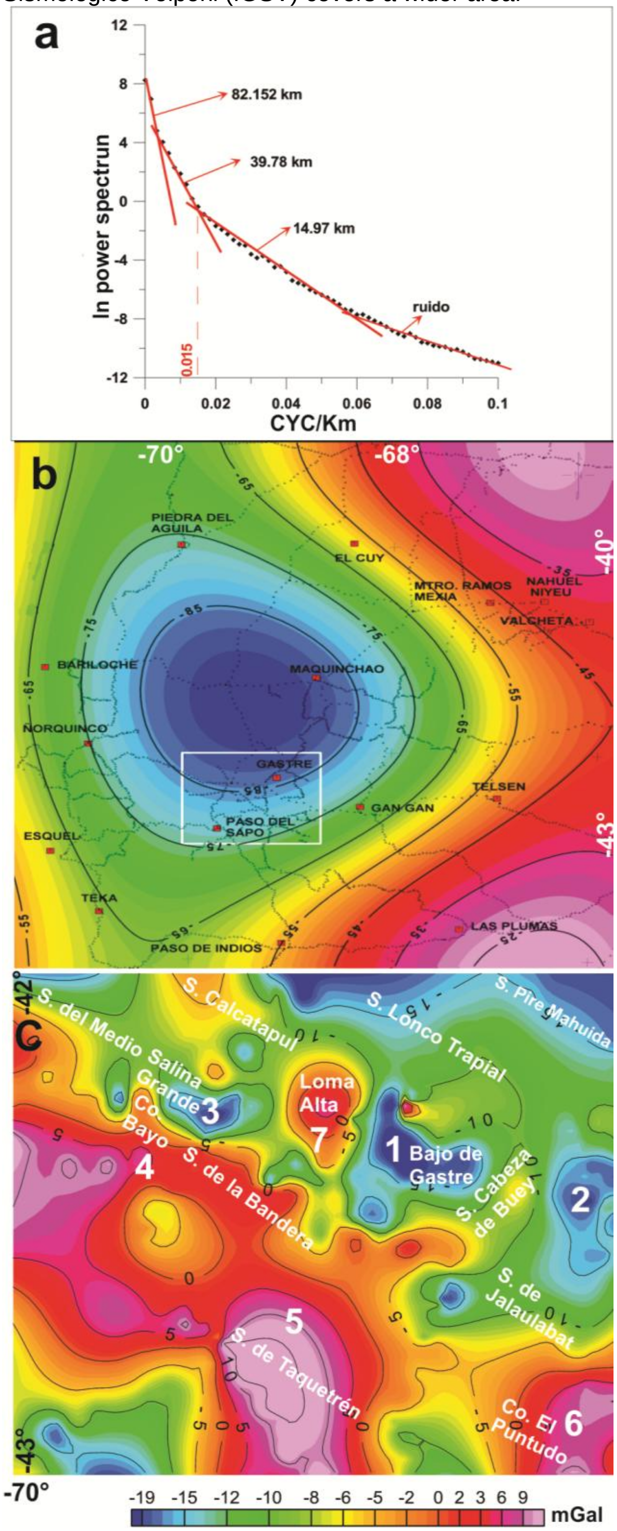

Figure 3: a) Radial power spectrum, b) Bouguer regional map, c) Bouguer residual map.

The radial power spectrum was obtained through the Oasis Montaj software vs 7.2 after reaching the North Patagonic Massif Bouguer map. In the radial power spectrum graphic (Figure 3a) three straight lines were identified. Each straight line slope is associated to one of average depth (Spector and Grand, 1970). The bigger slope is associated to mass anomalies on the upper mantle, the next one matches the regional anomaly (discontinuity mantle - crust) and is approximately 40 km, matches the data published by Christensen and Mooney (1995). The number of wave, which is 8, related to the second frequency spectrum breakage (0.015 cycles/km) was used as entrance parameter of a Butterworth filter. High frequency signals were filtered and only the low frequency ones or long length waves related to regional sources bigger than ~40 km deep remained. The Bouguer regional anomaly map (Figure 3b) is characterized by a minimum central gravimetric which matches the North-Patagonic Massif. Disregarding this Bouguer anomaly map regional tendency in the area of Gastre, the Bouguer residual map was obtained (Figure 3c). In order to highlight the lithologic contacts and considering the dominant direction of the trough, the gravity horizontal gradient was obtained perpendicularly (Figure 4).

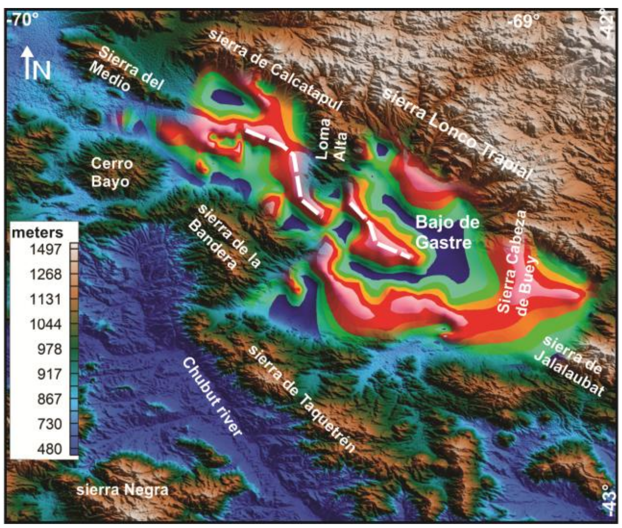

Figure 4: Gravity horizontal gradient map.

Magnetic data processing

The total magnetic field intensity values were corrected by diurnal variations. Trelew's magnetic observatory information was considered (red Intermagnet), records every minute. Later, to the corrected total magnetic field intensity map (Figure 5a), the IGRF field was deducted by the data acquisition date (Blakely, 1995), thus obtaining the corresponding magnetic anomalies to the study area (Figure 5a). The anomalies were reduced to the pole and overlapped to the residual gravimetric anomalies map, where there was a mismatch between the two signals. This absence of correlation is probably due to the existence of residual magnetization. Taking into consideration this latter, and that the shape of the analytical signal depends on the body position and not on the direction of the magnetization, the 3D analytical signal was applied; Roest et al., (1992). Lineaments that represent contact between lithofacies in Gastre were drawn using a digital elevation model of the terrain and the maxim of the 3D analytical signal (Figure 6a).

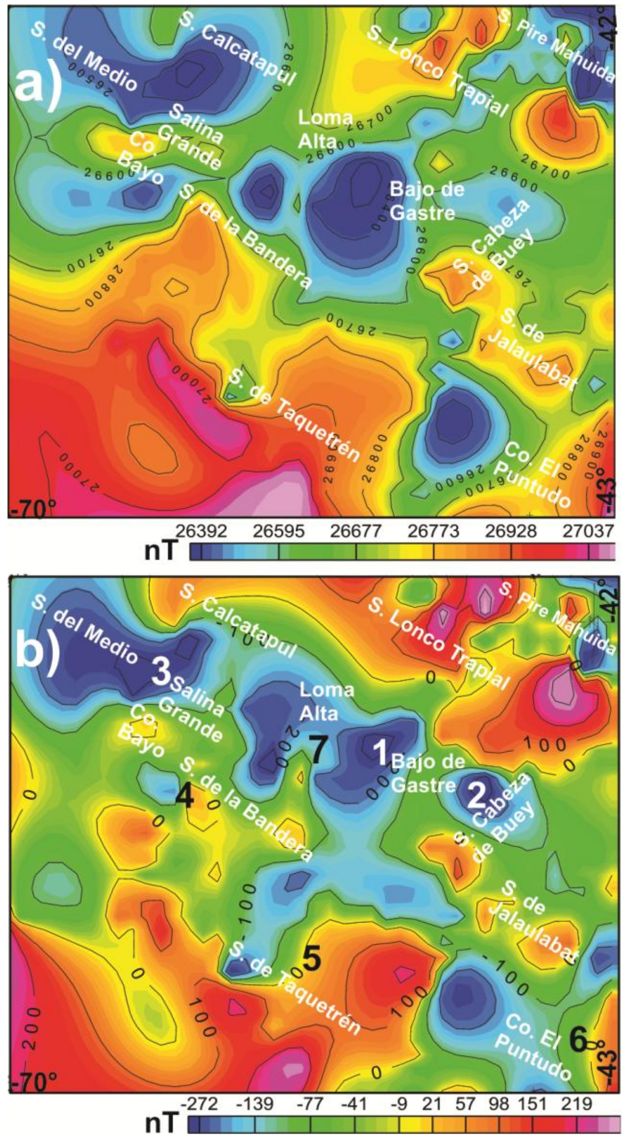

Figure 5: a) Map of total magnetic field intensity, b) Map of magnetometric anomaly. Map gridding every 3 km with the Minimum Curvature method.

Forward Modeling

i) Density calculation.

The densities of the different lithologic units which silt up the basin were obtained from a YPF.Ch.GF.es-1 record (Figure 7a). An appropriate statistical analysis was performed and the result was an average density value for each formation (Table 1). In terms of density values of the rocks that form the crystalline basement, sample surveys of the outcrops scattered across the area were performed (Figure 7c). Density values were established by double weighing method. Each measure displayed on Table 1 resulted of the average of 4 to 7 samples. The margin of error is one hundredth of unit. Then, taking into consideration that two-layer- density models will be made: a) sedimentary filling, and b) crystalline basement, a weighted average was performed setting each formation thickness that silts up the basin. A density of 2500kg m^{-3}

for the sedimentary filling was found (Table 2). For the crystalline basement, samples of different densities were averaged, the resulting value was 2700 kg $m^{-3.}$

ii) 2D Models of top crust

Three two-layered density models were built by using the GM SYS Program. Each layer was assigned a constant density value. A gravimetric answer was obtained from this model. Later, the difference between the observed data and the calculated response was minimized by the variation of the initial model density. To avoid the edge effect, the models spread over the edges of the profiles selected to model. The interpretation was based on the geological model introduced by Figari (2005) and LLambías et al., (1984). The adjustment error obtained between the calculated and observed anomalies was 0.2 mGal, and the uncertainty produced was of 10%.

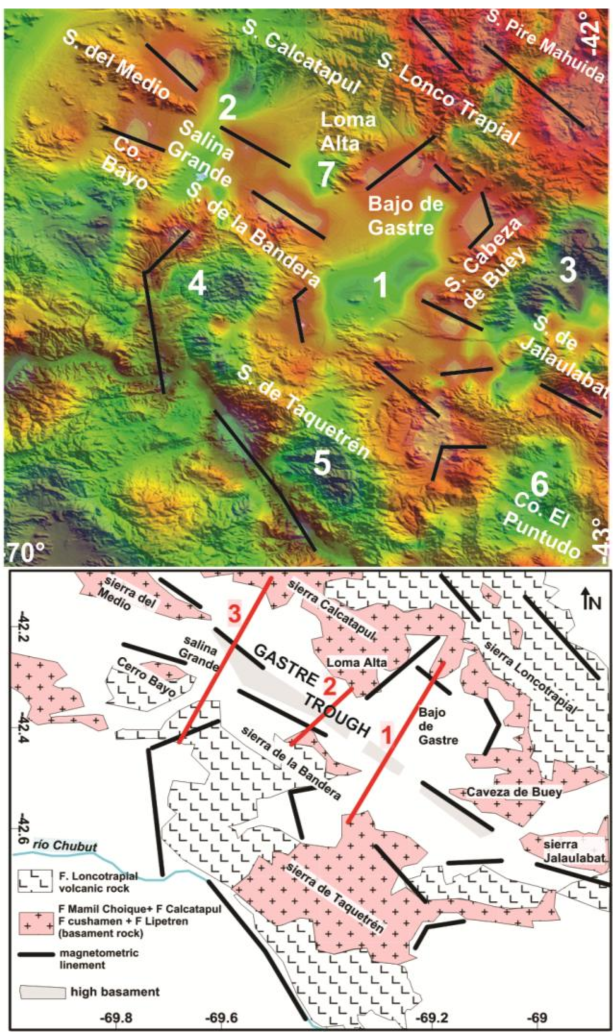

Figure 6: a) 3D analytical signal overlapped to DEM. b) Magnetic lineaments over geological map. Red lines show location of the density models. Shaded area shows high basement at central Gastre trough.

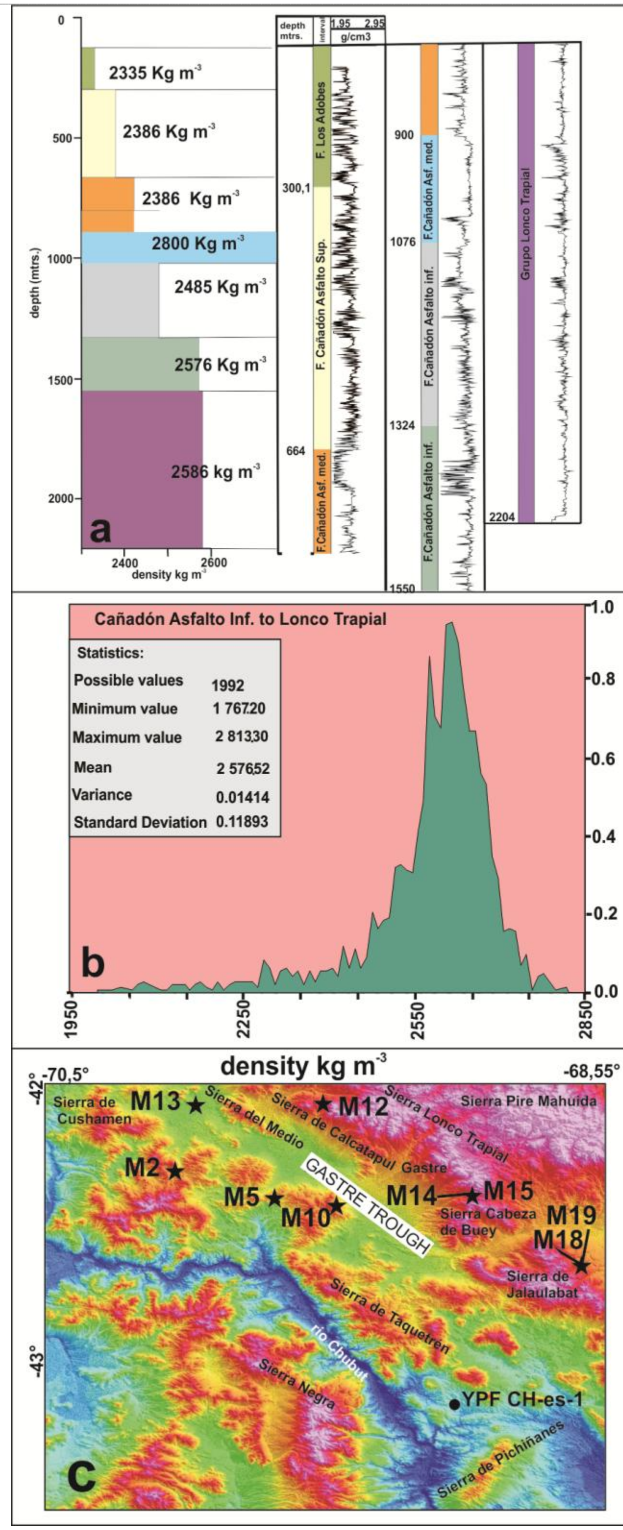

Figure 7: a) Outline of the distribution of densities found from the YPF.Ch.GF es-1 well record. b) Statistical curve that shows the medium density at lower Cañadón Asfalto - Lonco Trapial section, YPF.Ch.GF es-1. c) Places where basement samples were collected to determine their density.

Formation	location	Average Density (kg m^{-3})	Standard Deviation
Mamil Choique	M2	2760	0.002
	M5	2640	0.021
	M10	2650	0.001
	M12	2650	0.004
	M13	2800	0.006
Los Adobes	well	2335	0.092
Cañadón Asf. Sup.	well	2386	0.058
Cañadón Asf. Med	well	2386	0.048
Cañadón Asf. Med	well	2800	0.088
Cañadón Asf. Inf.	well	2485	0.096
Cañadón Asf. Inf. Inf.	well	2576	0.119
LoncoTrapial	well	2586	0.054

Table 1

z(m)	**e** (m)	**ρ** (kg m^{-3})	e* ρ	∆ **ρ** (kg m^{-3})
300	300	2335	700.5	2500
664	364	2386	868.504	
900	236	2386	563.096	
1076	176	2800	492.8	
1324	248	2485	616.28	
1550	226	2576	582.176	
2204	654	2586	1691.244	

Table 2

Results

In Bouguer residual map (Figure 3c) we can see over Gastre Trough three minimum gravimetrics of -15 mGal are developed. They are: 1) Bajo Gastre; 2) east of Cabeza de Buey Sierra, 3) Salina Grande (see numbering Figure 3c). All these minimums are divided by a high basement that develops in discontinuous way at central of Gastre Trough. The positive gravimetrics: 4) Sierra de la Bandera, 5) Taquetrén Sierra, 6) El Puntudo Hill, 7) Loma Alta, match the basement outcropping. In Paso del Sapo at Taquetrén Sierra we find the maximum gravity values, 12 mGal (Figure 3c). These values are interpreted as a high basement block through the Paso del Sapo failure during the Tertiary tectonic inversion stage.

In the map of magnetic anomalies, we can see closed iso anomalies associated to the same sources as Bouguer residual anomalies map. The edges of said sources are highlighted by the 3D analytical signal (Figure 6a). The magnetic lineaments marked from the analytical signal maximum values (Figure 6b) show contact between different lithologies as well as the map of gravity horizontal gradient (Figure 4). In these maps we can see the basement high at central Gastre Trough (Figure 6b).

The two-layered density models made at profiles 1, 2 and 3 (Figure 6b) shows the depth (~3600m) and the crystalline basement geometry at Gastre Trough (Figure 8). The results are consistent with the reported in Lince Klinger (2010) using the Frequency method and the deconvolution of Euler located at Gastre Trough.

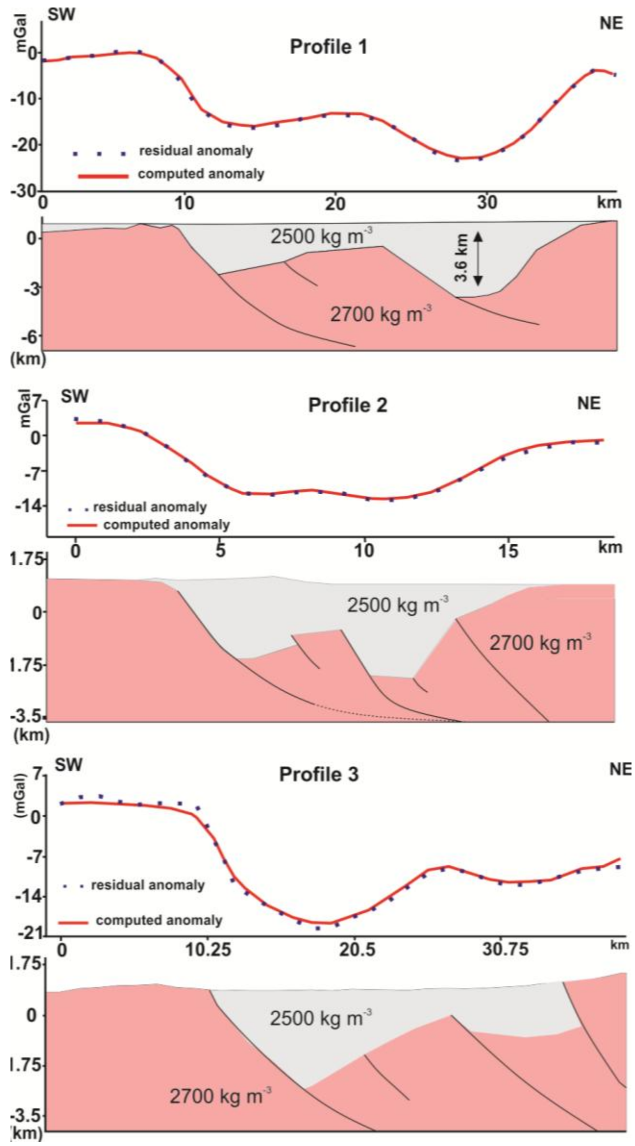

Figure 8: Density models

Conclusions

The gravimetric and magnetometric study performed at Gastre Trough allowed to know its basement geometry. The magnetism and gravity maps show a fractured basement with high and sunk blocks inside the trough.

The minimum anomalous are associated to graben-like depocenters probably inverted during the Tertiary. The maximum are linked to basement blocks, some outcropping on the trough edges and others covered by sediments inside. The 3D analytical signal and the horizontal gradient glimpse the existence of a high basement at central Gastre Trough. Said block seems to have been elevated during the Tertiary, due to the reactivation of older failures. Example of the latter is Sierra del Medio where the evidence is exposed.

Acknowledgments

The authors wish to thank CICITCA - UNSJ with the projects N° E816 - N° E815 and N° E810 for the contributions made, which partly helped to elaborate this piece of work.

References

Blakely, R. 1995. Potential theory in gravity and magnetic applications. Cambridge University Press: 441 p.

Christensen, N., Mooney, W. 1995. Seismic velocity structure and composition of the continental crust: A global view. *Journal Geophysical Research*, 100 (B7): 9761-9788.

Coira, B., Nullo, E., Proserpio, C. y Ramos, V. 1975. Tectónica del basamento en la región occidental del Macizo Nordpatagónico (prov. de Río Negro y Chubut). Republica Argentina. *Revista Asociación Geológica Argentina*, 30 (4): 361-383.

Cortiñas, J.S. 1996. La Cuenca Somún Curá – Cañadón Asfalto: Sus Límites, Ciclos evolutivos del relleno sedimentario y posibilidades exploratorias. XIII Congreso Geológico Argentino, Mendoza, Actas 1, 147-163.

Figari, E.G. y Courtade, S.F. 1993. Evolución tectosedimentaria de la Cuenca de Cañadón Asfalto, Chubut, Argentina. XII Congreso Geológico Argentino, Buenos Aires, Actas 1, 66 -77.

Figari, E.G. 2005. Evolución Tectónica de la Cuenca Cañadón Asfalto. (Zona del valle medio del río Chubut). Tesis Doctoral. Universidad de Buenos Aires. Facultad de Ciencias Exactas y Naturales, 106 p.

Hinze, W. J. 2003. Bouguer reduction density — Why 2.67 ? *Geophysics*, 68 (5): 1559–1560.

Hinze, W. J., C. Aiken, J. Brozena, B. Coakley, D. Dater, G. Flanagan, R. Forsberg, T. Hildenbrand, G. R. Keller, J. Kellogg, R. Kucks, X. Li, A. Mainville, R. Morin, M. Pilkington, D. Plouff, D. Ravat, D. Roman, J. Urrutia-Fucugauchi, M. V´eronneau, M. Webring and D. Winester., 2005. New standards for reducing gravity data: The North American gravity database. Geophysics, 70, 4, 125–132.

Lesta, P. J. 1968. Estratigrafía de la Cuenca del Golfo de San Jorge. III Jornadas Geológicas Argentinas, Buenos Aires, Actas, 1: 251-289.

Lesta, P. y Ferello, R. 1972. Región extra andina del Chubut y norte de Santa Cruz. Leanza A.F. (ed.) Geología Regional Argentina. Academia Nacional de Ciencias. Córdoba, 601-654.

Lince Klinger F. 2010. Estudio gravi-magnetométrico del Macizo Norpatagónico. Tesis doctoral. Universidad Nacional de San Juan. Facultad de Ciencias Exactas, Físicas y Naturales. 144 p (inédita).

LLambías, E. J., Llano, J. A., Rossa, N., Castro, C. E., Puidomenech, H. 1984. Petrografía de la Formación Mamil Choique en la Sierra del Medio – Departamento Cushamen – provincia del Chubut. IX Congreso Geológico Argentino , Actas 2, 554 – 567.

Morelli, C., Gantar, C., Honkasalon, T., McConnel, K., Tanner, J.G., Szabo, B., Uotila, U. y Whalen, C.T. 1974.The International Standardization Net 1971 (IGSN71), IUGG-IAG Publ. Spec. 4, *Int. Union of Geod. And Geophys*ics, Paris.

Nakayama, C., 1972. Informe geológico de la región comprendida entre la Sierra de Taquetrén y los Cerros Los Chivos y Negro de Marrauf, provincia de Chubut. YPF SA., inédito. Buenos Aires.

Proserpio, C. A. 1978. Descripción geológica de la hoja 42d, Gastre, Provincia del Chubut. Ministerio de Economía, Secretaria de Estado de Minería. Boletín 159. 1-75.

Rapela, W. C., Pankhurst, R. J. 1992. The granites of northern Patagonia and Gastre Fault System in relation to the break up of Gondwana, in: Storey, B.C., Alabaster, T., Pankhurst, R.J. (eds.) Magmatism and the Causes of Continental Break up. *Geological Society of London Special Publication*, 68: 209 – 220.

Rapela, W.C. 1997. El sistema de fallas de Gastre: e pur si muove. Argentina. *Revista de la Asociación Geológica Argentina*, 52 (2): 219 – 222.

Ravazzoli, I. A. y Sesana F. L. 1977. Descripción geológica de la hoja 41c-Río Chico. Servicio Geológico Nacional, Boletín 148:1-80.

Roest, W. R.; Verhoef, J. and Pilkington, M. 1992. Magnetic interpretation using the 3-D analytic signal. *Geophysics*, Vol. 57, (1): 116-125.

Spector, A. and Grant, F. 1970. Statistical models for interpreting aeromagnetic data. *Geophysics*, 35 (2):293 - 302.

Tasch, P. y Volkheimer W. 1970. Jurassic conchostracans from Patagonia. Paleontological Contributions, Kansas, 50: 1-23.

Volkheimer, W. 1964. Estratigrafía de la zona extra andina del departamento de Husmeen (Chubut), entre los paralelos de 42º y 42º 30’ y los meridianos 70º y 71º. *Revista Asociación Geológica Argentina*, 19(2): 85 -107.